

Available online at www.sciencedirect.com



Trans. Nonferrous Met. Soc. China 18(2008) 66-71

Transactions of Nonferrous Metals Society of China

www.csu.edu.cn/ysxb/

Synthesis and grain growth kinetics of in-situ FeAl matrix nanocomposites (II): Structural evolution and grain growth kinetics of mechanically alloyed Fe-Al-Ti-B composite powder during heat treatment

REN Rong(任榕), WU Yu-cheng(吴玉程), TANG Wen-ming(汤文明), WANG Feng-tao(汪峰涛), WANG Tu-gen(王涂根), ZHENG Zhi-xiang(郑治祥)

School of Materials Science and Engineering, Hefei University of Technology, Hefei 230009, China

Received 16 April 2007; accepted 16 July 2007

Abstract: Morphological changes, structural evolutions and grain growth kinetics of mechanically alloyed(MAed) $Fe_{50}AI_{50}$, $Fe_{42.5}AI_{42.5}Ti_5B_{10}$ and $Fe_{35}AI_{35}Ti_{10}B_{20}$ (mole fraction, %) powders were investigated by XRD and SEM, when being isothermally annealed at 1 073–1 373 K. The effect of different Ti and B addition on the grain growth of FeAl phase was also discussed. The results show that the nanocrystalline FeAl and in-situ TiB₂/FeAl nanocomposite powders can be synthesized by subsequent heat treatment. Besides the relaxation of crystal defects and lattice stress, the transformation from Fe-based solid solution into B2-FeAl and TiB₂ occurs upon heating of the MA-processed alloys. Although the grain growth takes place, the grain sizes of both FeAl and TiB₂ are still in nanometer scale. The activation energies for the nanocrystalline FeAl growth in the three alloys are calculated to be 534.9, 525.6 and 1 069.6 kJ/mol respectively, according to kinetics theory of nanocrystalline growth. Alloys with different TiB₂ contents exhibit unequal thermal stability. The presence of higher content TiB₂ plays significant role in the impediment of grain growth.

Key words: FeAl; composites; heat treating; structural evolution; grain growth kinetics

1 Introduction

In our previous work, powders composed of nanocrystalline Fe-based solid solution were obtained using a high-energy ball milling technique. However, for the industrial application, high temperature consolidation cannot be avoided in the production of high density bulk nano-materials from ball milled precursors [1-2]. Because of the large excess free energy, which is proportional to the specific grain boundary area, there is a high driving force for grain growth[3]. On the other hand, the choice of pressure and temperature for consolidation will strongly depend on the thermal stability of the nanocrystalline materials. Also, the potential structural application of nano-intermetallics at elevated temperatures will still require thermal stability at service temperatures. Therefore, the control of grain nano-intermetallics during growth in elevated temperature is the main task for improving of the properties as structural materials. In recent years, the thermal stability of nanostructured materials has received considerable attention, because grain growth and phase transformations will alter the properties of nanostructured materials during service or exposure of nanostructured materials to elevated temperatures. The grain growth can be limited by pinning the grain boundary with precipitates[4–6]. The in-situ reinforcement forming elements, such as Ti, B and C in the materials, may affect the final grain size by growth inhibition. In this work, the thermal stability of the nanocrystalline FeAl phase in different MAed Fe-Al-Ti-B systems was investigated in terms of the structural evolution, grain growth kinetics and micro-mechanism during annealing. A comparison of the calculated activation energies is made in order to understand the effect of Ti, B addition on FeAl grain growth kinetics of in-situ composites.

2 Experimental

Heat treatment was carried out by annealing the

Foundation item: Project(050440704) supported by the Natural Science Foundation of Anhui Province, China; Project(103-037016) supported by the Technological Innovation Foundation of Hefei University of Technology, China Corresponding author: WU Yu-cheng; Tel/Fax: +86-551-2905085; E-mail: ycwu@hfut.edu.cn MAed powders. The as-milled powders were separated by sieving and subjected in a GSL-1600X vacuum tubular type high-temperature furnace under a flowing argon atmosphere. In order to prevent oxidation, these powders were sealed into silica tubes, which were first evacuated, and then filled with pure argon. To study kinetics of grain growth of mechanically alloyed FeAl, isothermal annealing was carried out at 1 073, 1 173, 1 273 and 1 373 K for 1, 2 and 4 h at each temperature.

A Sirion200 type field emission gun scanning electron microscope(SEM) was used to analyze the morphological changes of the MAed and annealed powder. A D/max- γ B type X-ray diffractometer(XRD) with Cu K_a radiation (λ =0.154 nm) was used to characterize the structural evolutions of the powders during annealing. The average grain sizes of the phases were calculated by Scherrer formula, using standard method to eliminate the instrumental broadening contribution:

$$D = \frac{0.9\lambda}{B\cos\theta} \tag{1}$$

where λ is the wavelength of X-ray radiation, *B* is the angular width at half-maximum intensity and θ is the diffraction angle.

3 Results and discussion

3.1 Morphological evolution of powder particles after annealing

The SEM images of the 50 h milled Alloy 2 powders before and after heat treatment at 1 173 K for 4 h are shown in Fig.1. It is found that a uniform distribution of spherical powders with particle size of 2 um is obtained after 50 h of milling. Compared with Fig.1(a), the as-annealed powder particles intensely agglomerate, leading to the distributed size over a much wider range. As can be seen in Fig.1(b), some particle sizes increase to as large as 10 µm while some others are still 2-3 µm. The particle size distribution in mechanically alloyed powders is generally homogenous, for the outside force collision upon powder is from each direction during milling. While the particle size of powders in annealed materials is not only associated with the annealing temperatures and times, but also related to the microstructure. Well-knit powders in large aggregated particles are prone to grow up while it is difficult for small particles to grow. Thus, the size range becomes broader. To minimize the influences of different contact state of powders in agglomerate on structural evolution and grain growth behavior of annealed powder during annealing, MAed powders should be ground carefully to ensure powder particle size and composition of homogenization.

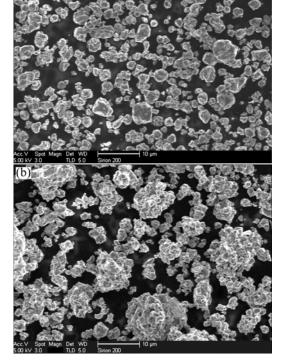


Fig.1 SEM images of 50 h milled Alloy 2 powders before (a) and after (b) heat treatment at 1 173 K for 4 h

3.2 Structural evolution at elevated temperatures

The final MAed products of Alloys 1, 2 and 3 are subjected to heat treating and then investigated by XRD. Different milling time is chosen for different samples because it is enough to obtain fully alloyed samples. Fig.2 shows the XRD spectra of the alloys milled for 30, 50 and 70 h respectively after annealing at 1 073-1 373 K for 4 h. XRD patterns of the 50 h milled Alloy 2 annealed at 1 373 K for 1-4 h are shown in Fig.3. From the patterns it can be seen that all peaks in Fig.2 become much sharper than those of milled powders before annealing and possess stronger intensity with rising annealing temperatures and time. The grain growth, internal strain elimination, lattice deformation reduction and lattice ordering degree increase processes may occur[7], which results in the shape change of the XRD pattern of MAed powder phases. In addition, no diffraction peaks of Fe-based solid solution but those of FeAl and TiB₂ are detected in the annealed powders. For all compositions it should be noted that the appearance of (100) and (111) superlattice reflections typical of the ordered B2 structure proves the ordering of Fe(Al)[8]. However, the details are different depending on the powder composition. For Alloy 3 milled for 70 h, more TiB₂ but few FeAl reflection peaks are detected, which indicates that the amount of FeAl phase in Alloy 3 is less

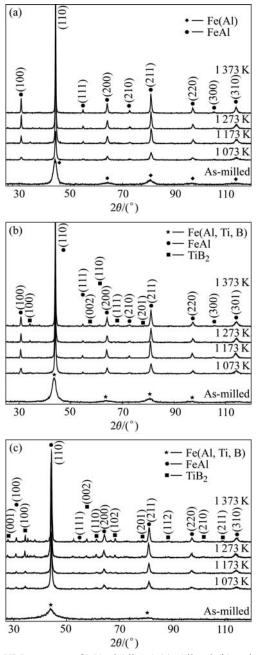


Fig.2 XRD patterns of MAed Alloy 1 (a), Alloy 2 (b) and Alloy 3 (c) annealed at 1 073, 1 173, 1 273 and 1 373 K for 4 h

than that in Alloy 1 and Alloy 2. From XRD patterns for the powders after higher temperature annealing (Fig.2(b)), the amount of TiB_2 compound increases with increasing the annealing temperature.

It is well known that mechanical alloying introduces large amount of defects such as vacancies, dislocations and grain boundaries into the as-milled powder. In the MAed powder, the lattice deformation is high, and the lattice ordering degree is low, which indicates that the powder is in non-equilibrium state. Annealing of as-milled alloys causes recovery of the defect structure. Atoms in the disordered or distorted positions rearrange and/or move into more thermodynamically equilibrated and

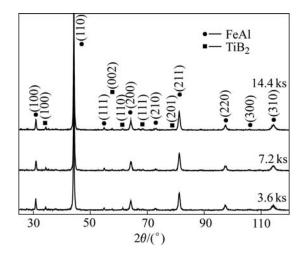


Fig.3 XRD patterns of 50 h milled Alloy 2 annealed at 1 373 K for different time

ordered or perfect lattice positions, enhancing the degree of ordering and strain release in the matrix. The heat treating of the MAed powder favors the diffusivity of Fe and Al. The decreasing of lattice deformation, and increasing of the lattice ordering degree result in the transformation from disordered Fe(Al) into ordered B2-FeAl intermetallic compound. Meanwhile, Ti and B precipitate from the non-equilibrium supersaturated Fe(Al, Ti, B) solid solution, and react to form hexagonal TiB₂ compound. Crystallization of the solid solution phase results in two-phase structure consisting of FeAl and TiB₂, which means both matrix phase and reinforcement phase are formed by in situ process. In addition, the high lattice deformation energy acts as the driving force for grain growth of the phases in MAed powder. This promotes the grain growth of FeAl and TiB₂ during heat treatment. Although the grain size of all alloys increases with increasing the annealing time or temperature, the alloys maintain the nano-sized grains up to the annealing temperature of 1 373 K at an annealing time of 4 h.

3.3 Grain growth kinetics of nanocrystalline FeAl phase during annealing

The parabolic law of the grain growth proposed by BURKE and TURNBULL was earlier used to describe the grain growth characteristics under the condition of heat treatment, but it is limited in the temperature range near the melting point[10]. So, a general grain growth equation was then developed to substitute it, which is described as[9–10]

$$D^n - D_0^n = Kt \tag{2}$$

where D is the grain size at a given annealing time; D_0 is the initial grain size; t is the heat treatment time; n is

the grain growth exponent, and K is the grain growth rate constant. If atomic diffusion across the grain boundary is a simple activated process, the grain growth rate constant K in an Arrhenius form can be written as

$$K = K_0 \exp[-Q/(RT)] \tag{3}$$

where K_0 is the pre-exponential term; Q is the activation energy for grain growth; T is the absolute temperature of annealing and R is the gas constant. Eqn.(2) is usually reduced on the assumption that D is much greater than D_0 :

$$D^n = Kt \tag{4}$$

$$n \lg D = \lg K + \lg t$$
 (5)

However, as observed experimentally (Fig.2), the fact that D of FeAl phase after annealing for 4 h is still not large enough to neglect D_0 . In this case, Eqn.(5) can be handled as[11]

$$\lg \frac{\mathrm{d}D(t)}{\mathrm{d}t} = -(n-1)\lg D(t) + \lg K - \lg n \tag{6}$$

Therefore, the plot of the logarithm dD(t)/dt against the logarithm D(t) should give a slope of n-1. According to the combination of Eqns.(2) and (3),

$$D^{n} - D_{0}^{n} = K_{0} \{ \exp[-Q/(RT)] \} t$$
(7)

In addition, Eqn.(7) can be rewritten as

$$\lg[(D^{n} - D_{0}^{n})/t] = \lg K_{0} + [-Q/(RT)\lg e]$$
 (8)

According to Eqn.(8), if *n* is known, *Q* can be inferred from the plot of $lg[(D^n - D_0^n)/t]$ versus 1/T.

The kinetics of grain growth was studied in FeAl phase of all three alloys. Grain sizes obtained from XRD patterns are plotted as a function of annealing temperature in Fig.4 for three alloys. The grain growth data are fitted to Eqn.(6) using a non-linear fitting route. The growth rate dD(t)/dt is then obtained by taking the tangent on the isothermal curve at 1, 2 and 4 h. The variation of the grain size with the annealing time follows a similar course, i.e. a nearly parabolic increase with increasing annealing time. For an annealing time of 1 h a sharp increase in the grain size is apparent, while for longer annealing time (≥ 2 h) the grain size does not change significantly. This drop in the growth rate arises because of the decrease of the interfacial energy as the grain size increases[9]. And the decrease of the interfacial energy will reduce the driving force for a grain growth process and then stabilize the grain size. In addition, when the temperature raises, the grain growth increases. From Fig.4, Alloy 3 appears to offer an improvement in stability relative to Alloy 1 and Alloy 2.

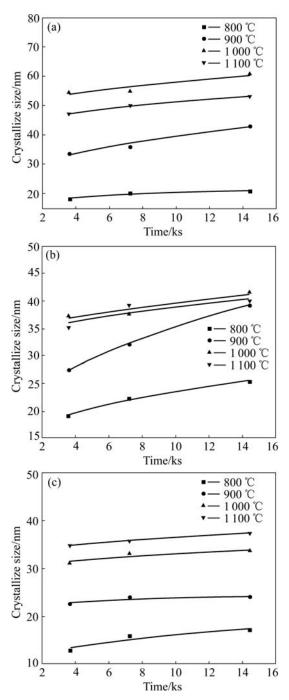


Fig.4 Grain growth curves in isothermal annealing of MAed Alloy 1 (a), Alloy 2 (b) and Alloy 3 (c) annealed at 1 073–1 373 K for 1–4 h

In a comparison of the grain growth behavior of three alloys, it can be observed that the grain sizes of FeAl in Alloy 1 are always the largest, while those in Alloy 3 are the finest among the three alloys. For example, after heat treating at 1 173 K for 1 h, the grain sizes of FeAl are 36.2, 28.9 and 22.7 nm respectively. And the increase of the grain size in Alloy 3 is significantly smaller than that in both Alloy 1 and Alloy 2. For the samples, the growth tendency of FeAl

decreases with the increase of TiB_2 content. This hinderence can be explained by in-situ formation of fine TiB_2 particles that may result in pinning of grain boundaries, which indicates that the addition of Ti and B can restrain the growth of grain size. Thus, Ti and B are found to be beneficial for grain refinement at higher concentrations both in milling and annealing.

Recent studies have shown that the values of *n* vary depending on the grain growth mechanism. For normal grain growth in a pure single-phase system, when n=2, the grain growth process is usually the curvature-driven migration of grain boundaries in pure materials; if n=4, the process is the stochastic jumping of atoms across the grain boundaries; and n=3, the process is controlled by volume diffusion[6]. As observed experimentally[12-13], *n* is usually larger than 2, and covers a range from 2 to 5 corresponding to various metallic systems and temperature ranges. The values of n obtained in Eqn.(6) are listed in Table 1 for each temperature of each alloy. An increase in value of n with increasing annealing temperature is noted. The n values are very large compared with those normally found, indicating that the kinetics is very complicated in a nanocrystalline multiphase system.

Table 1 Calculated grain growth exponent n of FeAl inpowders annealed at different heat treatment temperatures

1			1
Annealing	Grain growth exponent <i>n</i>		
temperature/K	Alloy 1	Alloy 2	Alloy 3
1 073	5.3	3.5	3.3
1 173	3.7	2.6	10.5
1 273	6.1	5.9	9.1
1 373	6.9	5.7	10.4

Eqn.(8) indicates that, when $lg[(D^n - D_0^n)/t]$ is plotted as a function of 1/T for FeAl phase, the data points can be expected to lie on a straight line. Fig.5 shows such three plots. Three straight lines can be drawn, and from their slopes, the activation energies for grain growth of FeAl phase in three alloys can be estimated as 534.9, 525.6 and 1 069.6 kJ/mol, respectively (Table 2). However, the present values of Q are quite higher than the activation energies for processes associated with grain growth (the activation energies for self diffusion of pure Fe (251-282 kJ/mol) and pure Al (142 kJ/mol), the activation energy for lattice diffusion of Fe (174 kJ/mol) in pure Fe[14-15] and the activation energies for lattice diffusion of Fe (265 kJ/mol) and Al (258 kJ/mol) in B2-FeAl[16]). The large increase in the activation energy of MAed powder appears to be related to the homogeneously dispersing of Al or Al, Ti and B in Fe lattice during the mechanical alloying. Besides, the

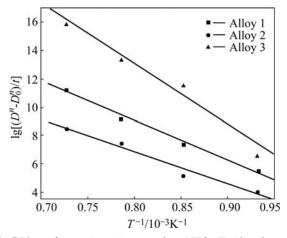


Fig.5 Plots of $lg[(D^n - D_0^n)/t]$ against 1/T for FeAl grains

 Table 2 Calculated activation energies required for grain growth of FeAl grains

Alloy	Activation energy $Q/(kJ \cdot mol^{-1})$	
1	534.9	
2	525.6	
3	1069.6	

in-situ formation of TiB_2 has the effect of reducing the grain growth rate of FeAl matrix by pinning of grain boundaries during annealing.

The grain sizes of FeAl (13-61 nm) and TiB_2 (15-43 nm) in the three alloys after annealing indicate that the nanocrystalline FeAl and in-situ TiB₂/FeAl nanocomposite have a high thermal stability.

4 Discussion

Previous studies on the thermal stability of nanocrystals in mechanically alloyed nanocrystalline materials have shown the complicated character of grain growth. The inhibition of grain growth in MAed materials is not only associated with the grain boundary segregation, solute (impurity) pinning, second-phase (Zener) pinning and remnant pore pinning, but also related to the changing level of strain and the degree of ordering. These factors, therefore, affect the grain growth kinetics of MAed nanocrystalline materials. Reflecting in the grain growth kinetics of MAed nanocrystals, the grain growth may be operated by at least one mechanism occurring simultaneously. For example, the grain growth process of the nanocrystalline Fe seems to be governed by two different mechanisms[14].

Although the grain growth in the nanocrystalline FeAl is controlled by atomic diffusion at grain boundary, this process can be controlled by the effects of other factors. In this work, the following factors might play an important role in grain size stability. Al, Ti and B atoms supersaturated diffuse into Fe lattice during mechanical alloying, leading to the lattice distortion and the impediment of dislocation glide and dynamic recrystallization. Nano-grains in the MA-processed alloys are very stable for the intrinsic factors, such as random orientation of neighboring grains or reorientation of random atoms in disordered grain boundaries[17]. For the starting as-milled powders, considering the non-equilibrium process by which the as-milled powders are prepared, Al, Ti and B solutes at grain boundaries may hinder grain growth until high temperature annealing. The in-situ formation of the second-phase particles TiB₂ may result in the inhibition of grain growth. The stabilizing effect can be related to TiB₂ precipitation and the grain boundary pinning effect of these particles.

In order to estimate the effect of TiB₂ phase on grain growth in the three alloys, the activation energies for grain growth of FeAl phase in Alloys 1, 2 and 3 obtained in the present work are compared. The O for grain growth of FeAl phase in Alloy 2 is close to that of Alloy 1, whereas Q for grain growth of FeAl phase in Alloy 3 is substantially higher than that of Alloy 1 and Alloy 2. The analysis indicates that the different TiB₂ addition has different effect on the grain growth in the alloys, which means alloys with different TiB₂ contents exhibit unequal thermal stability. The reason for that is not clear. One most possible reason for this phenomenon is the presence of high content TiB_2 in Alloy 3. Although the secondary TiB₂ phase appears at the annealing process in Alloy 2, the grain growth kinetics in Alloy 2 and Alloy 1 is almost the same. Thus the low content of TiB₂ phase has little effect on the grain growth of FeAl in Alloy 2. It is notable that the presence of the high content TiB₂ plays significant role in the impediment of grain growth. The enhanced grain size stability due to a high content of TiB₂ needs more detailed investigations, which are in progress.

5 Conclusions

1) Nanocrystalline FeAl and in-situ TiB₂/FeAl nanocomposite powders can be synthesized by mechanical alloying and subsequent heat treatment process.

2) Besides the relaxation of crystal defects and lattice stress, the transformation from Fe-based solid solution into B2-FeAl and TiB₂ occurs upon heating of the MA-processed alloys. Although the grain growth takes place, the grain sizes of both B2-FeAl and TiB₂ are still in nanometer scale. And the grain size decreases with increasing TiB₂ content.

3) The grain growth exponent n of nanocrystalline FeAl in the three alloys increases with isothermal

annealing from 1 073 to 1 373 K. The grain growth of FeAl is significantly inhibited especially at elevated temperatures.

4) The activation energies for nanocrystalline FeAl in the three alloys are determined to be 534.9, 525.6 and 1 069.6 kJ/mol respectively, in isothermal annealing from 1 073 to 1 373 K. Alloys with different TiB₂ contents exhibit different thermal stability. The presence of higher content TiB₂ plays an significant role in the impediment of grain growth.

References

- KRASNOWSKI M, WITEK A, KULIK T. The FeAl-30%TiC nanocomposite produced by mechanical alloying and hot-pressing consolidation [J]. Intermetallics, 2002, 10: 371–376.
- [2] KRASNOWSKI M, KULIK T. FeAl-TiN nanocomposite produced by reactive ball milling and hot-pressing consolidation [J]. Scripta Materialia, 2003, 48: 1489–1494.
- [3] GROZA J R. Nanosintering [J]. Nanostruct Mater, 1999, 12: 987–992.
- [4] SENKOV O N, CAVUSOGLU M, FROES F H. Synthesis and characterization of a TiAl/Ti₅Si₃ composite with a submicrocrystalline structure [J]. Mater Sci Eng A, 2001, 300: 85–93.
- [5] CHENG J S, CHEN H B, YANG B, FAN J Z, TIAN X F, ZHANG J S. Preparation of bulk nanocrystalline Al-Zn-Mg-Cu alloy with high thermal stability by cryomilling [J]. The Chinese Journal of Nonferrous Metals, 2006, 16(7): 1196–1201. (in Chinese)
- [6] LU L, TAO N R, WANG L B, DING B Z, LU K. Grain growth and strain release in nanocrystalline copper [J]. J Appl Phys, 2001, 89(11): 6408–6414.
- [7] MURTY B S, RANGANATHAN S. Novel materials synthesis by mechanical alloying/milling [J]. Int Mater Rev, 1998, 43: 101–141.
- [8] FAN R H, SUN K N, YIN Y S, BAO Z C. Synthesis of iron aluminides from elemental powders by mechanical alloying [J]. Chinese Journal of Mechanical Engineering, 2000, 36(8): 55–58. (in Chinese)
- [9] GIL F J, PLANELL J A. Behavior of normal grain growth kinetics in single phase titanium and titanium alloys [J]. Mater Sci Eng A, 2000, 283: 17–24.
- [10] KAMARA M, UENISHI K, KOBAYASHI K F. Nano-structured intermetallic compound TiAl obtained by crystallization of mechanically alloyed amorphous TiAl, and its subsequent grain growth [J]. J Mater Sci, 2000, 35: 2897–2905.
- [11] ROCK C, OKAZAKI K. Grain growth kinetics and thermal stability in a nanocrystalline multiphase mixture prepared by low-energy ball milling [J]. Nanostruct Mater, 1995, 5(6): 657–671.
- [12] CAO P, LU L, LAI M O. Grain growth and kinetics for nanocrystalline magnesium alloy produced by mechanical alloying [J]. Mater Res Bul, 2001, 36: 981–988.
- [13] ZHOU L Z, GUO J T. Grain growth and kinetics for nanocrystalline NiAl [J]. Scripta Mater, 1999, 40(2): 139–144.
- [14] MALOW T R, KOCH C C. Grain growth in nanocrystalline iron prepared by mechanical attrition [J]. Acta Mater, 1997, 45(5): 2177–2186.
- [15] SHAW L, LUO H, VILLEGAS J, MIRACLE D. Thermal stability of nanostructured Al₉₃Fe₃Cr₂Ti₂ alloys prepared via mechanical alloying [J]. Acta Mater, 2003, 51: 2647–2663.
- [16] MEHRER H, EGGERSMANN M, GUDE A. Diffusion in intermetallic phases of the Fe-Al and Fe-Si systems [J]. Mater Sci Eng A, 1997, 239/240: 889–898.
- [17] LIU K W, MUCKLICH F. Thermal stability of nano-RuAl produced by mechanical alloying [J]. Acta Mater, 2001, 49: 395–403.

(Edited by LI Xiang-qun)